Short communication

Phase and microstructure stabilities of LiAlO$_2$ in molten Li/Na carbonate for molten carbonate fuel cells

S.D. Kim[a], S.H. Hyun[a,*], M.Y. Shin[a], T.H. Lim[b], S.A. Hong[b], H.C. Lim[c]

[a] *School of Advanced Materials Science and Engineering, College of Engineering, Yonsei University, Seoul 120-749, Republic of Korea*
[b] *Battery and Fuel Cell Research Center, KIST, Seoul 136-791, Republic of Korea*
[c] *Korea Electric Power Research Institute, Yuseong-gu, Daejeon 103-16, Korea*

Abstract

The phase and microstructure stabilities of LiAlO$_2$ for improving the matrix reliability of molten carbonate fuel cells are investigated. The phase transformation and particle growth of LiAlO$_2$ are examined via immersion tests of pure γ-LiAlO$_2$, an α-/γ-LiAlO$_2$ mixture and pure α-LiAlO$_2$ in molten carbonate at 650 °C in an air atmosphere. Dissolution of Li$^+$ ions occurs mainly from γ-LiAlO$_2$ over an 18 000 h period, and the dissolved Li$^+$ ions precipitate as LiNaCO$_3$ and α-LiAlO$_2$. Particle growth takes place continuously from an early stage of heat-treatment and quickly progresses by the accelerated dissolution and precipitation of Li$^+$ ions after 10 000 h. By contrast, the particle size and the crystalline phase of α-LiAlO$_2$ do not change during 3000 h of immersion. These results show that α-LiAlO$_2$ is less soluble than γ-LiAlO$_2$ and is more stable in molten carbonate.
© 2005 Elsevier B.V. All rights reserved.

Keywords: Molten carbonate fuel cell; LiAlO$_2$ electrolyte matrix; Phase transformation; Particle growth; Solubility; Stability

1. Introduction

The electrolyte matrix of the molten carbonate fuel cell (MCFC) is used for electronic insulation and ionic (CO$_3^{2-}$) communication between the electrodes. In a porous plate manufactured from LiAlO$_2$ powder, the electrolyte matrix is comprised of the molten carbonate, which is solid at room temperature and paste-like at the operation temperature of 650 °C. The performance of the unit cell is affected mainly by the amount of molten carbonate in the matrix [1]. The electrolyte matrix is required to have, high porosity (50–70%) and a sharp pore-size distribution (0.1–0.3 μm) for stable electrolyte retention by capillary action.

The molten carbonate is so corrosive at the high temperature of 650 °C that the degradation of the cell components can easily occur. Pore coarsening of the matrix by particle growth and phase transformation of LiAlO$_2$ is the main reason for electrolyte depletion [2]. To date, γ-LiAlO$_2$ is used for MCFC matrix materials due to its high corrosion resistance to molten carbonate electrolytes, and reinforcement with rod-shaped γ-LiAlO$_2$ particles has been proposed for elimination of the structural and chemical weakness of MCFC electrolyte matrices [3–8]. In recent years, however, it has been observed that γ-LiAlO$_2$ undergoes particle growth, and that the crystal phase of LiAlO$_2$ in the matrix is transformed from γ-LiAlO$_2$ to α-LiAlO$_2$ during MCFC operation [9,10].

The current study examines the long-term stability of LiAlO$_2$ in molten carbonate at 650 °C in an air atmosphere for up to 18 000 h. Observation are made of the elution and the dissolution of LiAlO$_2$ and a possible explanation is given for the particle growth and phase transformation of LiAlO$_2$.

* Corresponding author. Tel.: +82 2 2123 2850; fax: +82 2 365 5882.
  E-mail address: prohsh@yonsei.ac.kr (S.H. Hyun).

2. Experimental

The microstrcuture change and phase transformation of $LiAlO_2$ were investigated by immersion tests. Two allotropes of $LiAlO_2$ were used, namely: α-$LiAlO_2$ (Cyprus Foot Mineral Co. Ltd., surface area $= 10\,m^2\,g^{-1}$, density $= 3.40\,g\,cm^{-3}$) and γ-$LiAlO_2$ (HAS-10, Cyprus Foot Mineral Co. Ltd., surface area $= 10\,m^2\,g^{-1}$, density $= 2.61\,g\,cm^{-3}$). β-$LiAlO_2$ was excluded because it had been reported that the material is unstable in molten carbonate [1,2]. The carbonate mixture, which melts at 650 °C via an eutectic reaction, was prepared from, $Li_2/Na_2CO_3 = 52/48$ molar ratio. The immersion tests were performed in an air atmosphere at selected times over a 18 000 h period at 650 °C in alumina crucibles that contained pure γ-$LiAlO_2$, or an α-/γ-$LiAlO_2$ mixture with molten carbonate. The stability of pure α-$LiAlO_2$ over 3000 h was also estimated by the same method. Sample washing and examination was performed at selected times: namely: initially and then, 200, 500, 1000, 2000, and 3000 h. Each specimen was prepared by eliminating the residual molten carbonate in $LiAlO_2$ with a washing solution (1:1:2 = acetic acid:acetic anhydride:methanol in molar ratio) and then dried.

The crystalline phases of $LiAlO_2$ were analyzed by X-ray diffractometry (Rint 2700, Rigaku Co., Tokyo, Japan). The particle growth and surface-area variation of each specimen were measured by a dynamic laser scattering (DLS) method using a particle-size analyzer (Par III, Otsuka Electronics Co., Japan) and BET equipment (Gemini 2375, Micromeritics, USA), respectively. The microstructure changes of the specimen were observed by scanning electron microscopy (S4200, Hitachi, Ltd., Tokyo, Japan).

3. Results

3.1. Crystalline phase change of $LiAlO_2$

The crystalline phase of pure γ-$LiAlO_2$ in molten carbonate (Li_2/Na_2CO_3) at 650 °C in an air atmosphere is given in Fig. 1. The elution of $LiNaCO_3$ takes place during the early stage of heat-treatment, but the phase transformation of γ-$LiAlO_2$ does not occur during 18 000 h. A comparison of the phase stability of α-$LiAlO_2$ and γ-$LiAlO_2$ from an immersion test of an α-/γ-$LiAlO_2$ mixture in molten carbonate at 650 °C in an air atmosphere is given in Fig. 2. With the passage of the time, the XRD data show that large amounts of $LiNaCO_3$ are precipitated out, and the intensity of γ-$LiAlO_2$ decreases gradually. By contrast, the crystalline phase of α-$LiAlO_2$ is stable and remains unchanged during the heat-treatment time.
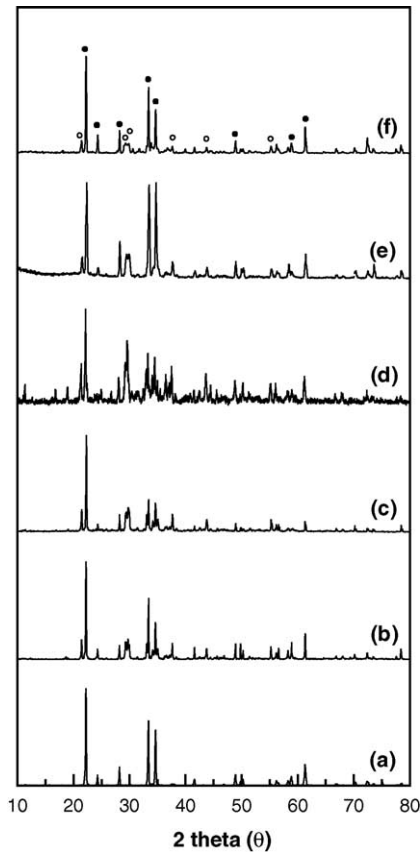

Fig. 1. XRD patterns for γ-$LiAlO_2$ particles treated with molten carbonate at 650 °C: (a) initial, (b) 3000, (c) 7000, (d) 11 000, (e) 14 000 and (f) 18 000 h. (●): γ-$LiAlO_2$; (○): $LiNaCO_3$.
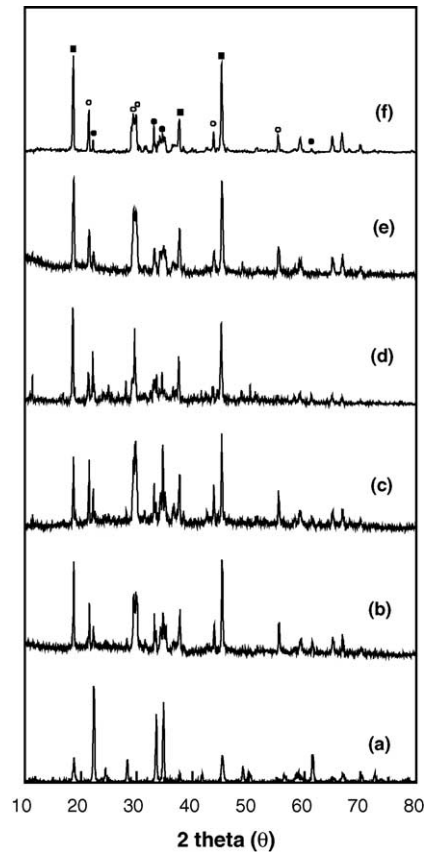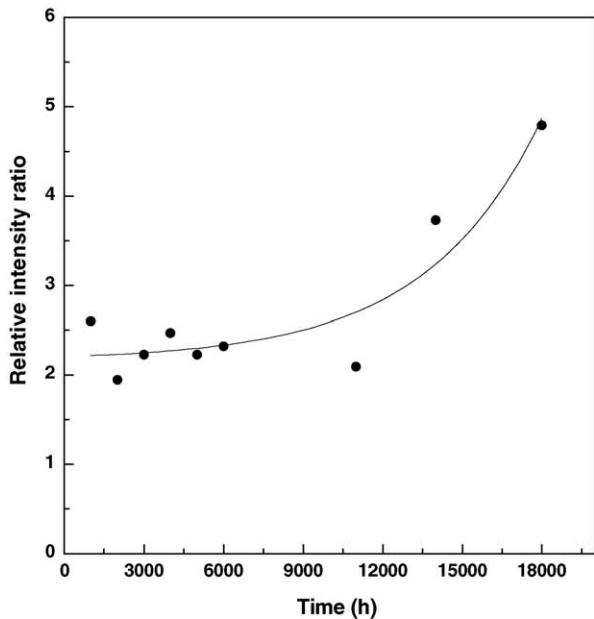

Fig. 2. XRD patterns for α-/γ-$LiAlO_2$ mixture (1:1) treated with molten carbonate at 650 °C: (a) initial, (b) 3000, (c) 7000, (d) 11 000, (e) 14 000, and (f) 18 000 h. (■): α-$LiAlO_2$; (●): γ-$LiAlO_2$; (○): $LiNaCO_3$.

Fig. 3. Variation with heat-treatment time of the relative intensity ratio of for α-LiAlO$_2$ over γ-LiAlO$_2$ from an α-/γ-LiAlO$_2$ mixture (1:1) treated with molten carbonate at 650 °C.

These phenomena are analyzed quantitatively in Fig. 3, which shows the relative intensity ratio of α-LiAlO$_2$ over γ-LiAlO$_2$ from XRD analysis of the α-/γ-LiAlO$_2$ mixture with heat-treatment time. The ratio gradually increases up to 10 000 h
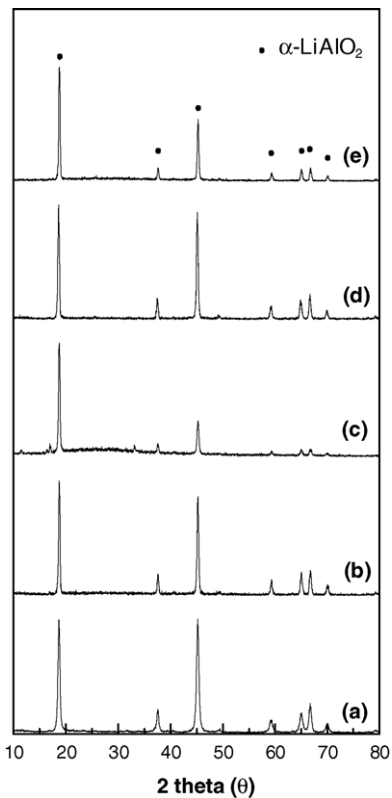

Fig. 4. XRD patterns for pure α-LiAlO$_2$ treated with molten carbonate at 650 °C: (a) initial, (b) 200, (c) 500, (d) 2000 and (e) 3000 h.
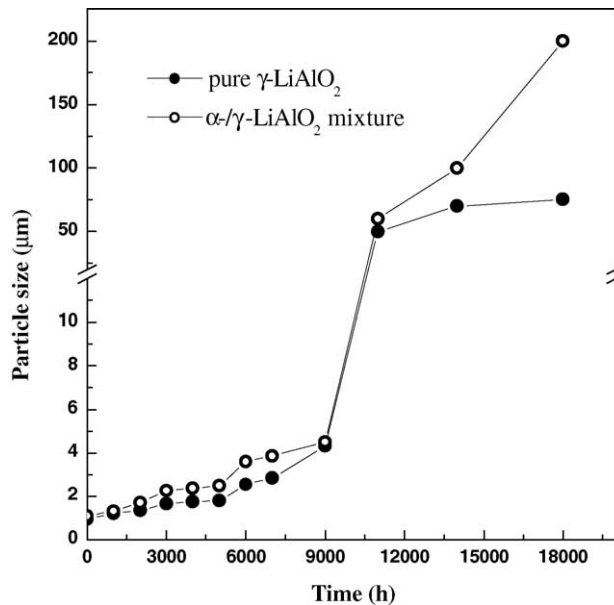

Fig. 5. Particle size variations of LiAlO$_2$ treated with molten carbonate at 650 °C as a function of heat-treatment time.

and then suddenly accelerates. Pure α-LiAlO$_2$, as depicted in Fig. 4, is very stable in the molten carbonate after 3000 h, and it is worth noting that there is no elution of LiNaCO$_3$ as is seen for pure γ-LiAlO$_2$ and an α-/γ-LiALO$_2$ mixture.

3.2. Particle growth of LiAlO$_2$

Variation of the particle size of pure γ-LiAlO$_2$ and an α-/γ-LiAlO$_2$ mixture with heat-treatment time is given in Fig. 5. The particle size of each specimen increases gradually up to
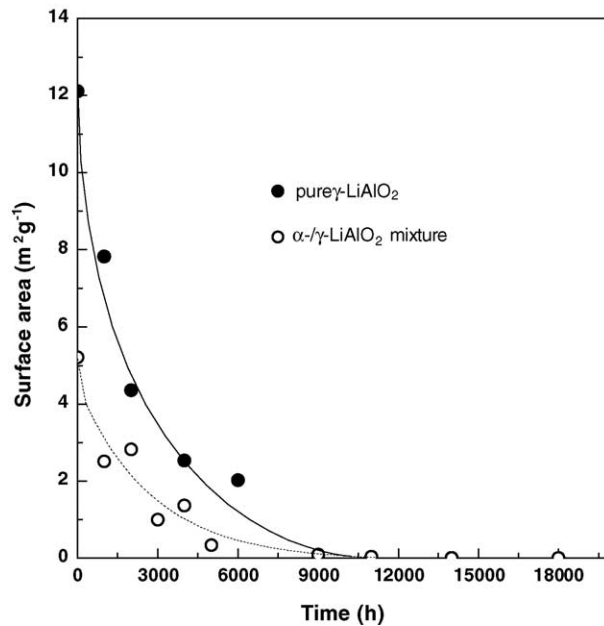

Fig. 6. Variation of surface area of LiAlO$_2$ treated with molten carbonate at 650 °C as a function of treatment time.
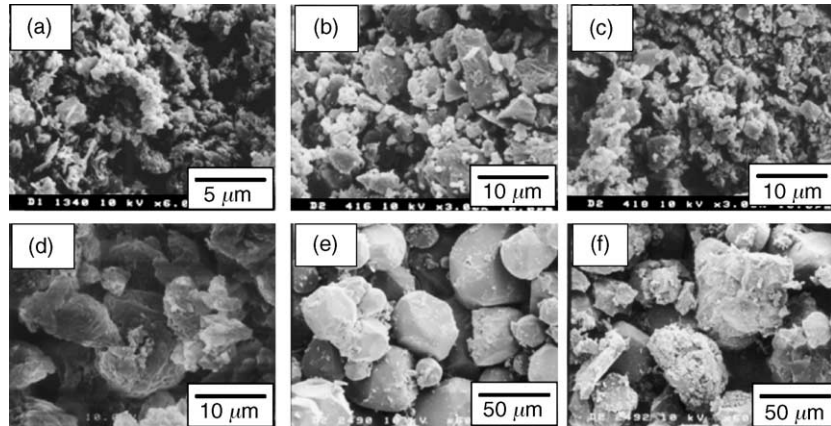
Fig. 7. Microstructure variations of pure γ-LiAlO$_2$ treated with molten carbonate at 650 °C: (a) initial, (b) 3000, (c) 7000, (d) 9000, (e) 11 000 and (f) 14 000 h.
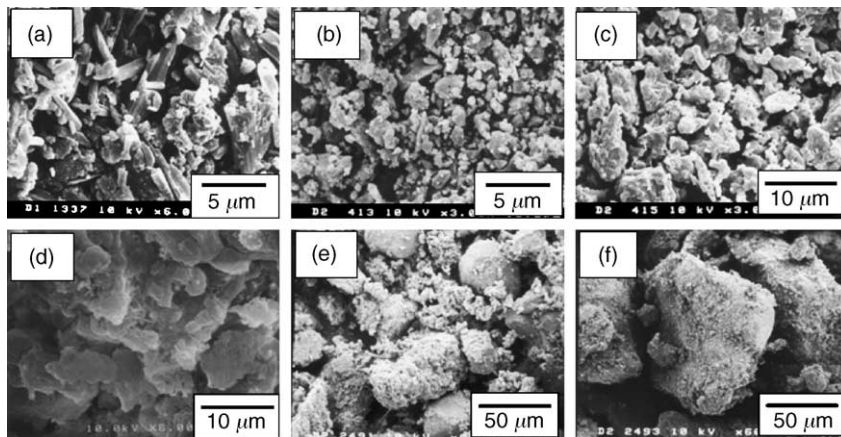

Fig. 8. Microstructure variations of α-/γ-LiAlO$_2$ mixture treated with molten carbonate at 650 °C: (a) initial, (b) 3000, (c) 7000, (d) 9000, (e) 11 000 and (f) 14 000 h.
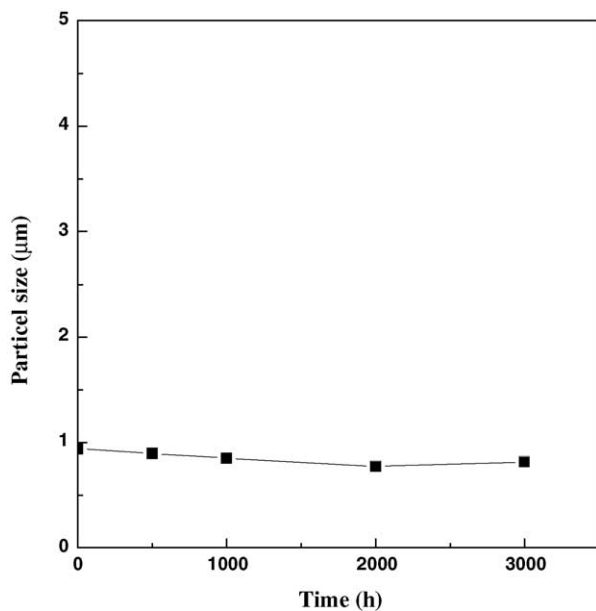

Fig. 9. Particle size variations of α-LiAlO$_2$ treated with molten carbonate at 650 °C as a function of treatment time.

10 000 h and then rapidly there after. The specific surface-area of each sample decreases to an undetectable value after 10 000 h (see Fig. 6) when suddenly the particle growth rate of α-/γ-LiAlO$_2$ becomes greater than that of γ-LiAlO$_2$. The scanning electron micrographs in Figs. 7 and 8 show that the particles grow continuously and that their surfaces become smoother with heat-treatment time. In the case of pure α-LiAlO$_2$, however, the particle size is maintained at a constant value (1 μm), and the microstructure does not change during the 3000 h immersion test (Figs. 9 and 10). The surface area decreases in the initial stages of heat-treatment and decreases to almost zero after 500 h (Fig. 11).

4. Discussion

The stability of LiAlO$_2$ has been investigated by means of immersion tests of pure γ-LiAlO$_2$, an α-/γ-LiAlO$_2$ mixture, and pure α-LiAlO$_2$. Reasonable explanations for the phase transformation and particle growth of LiAlO$_2$ are presented by the analysis of 18 000 h of experiments.

The phase stability of LiAlO$_2$ in molten carbonate at the MCFC operation temperature (650 °C) is generally evaluated
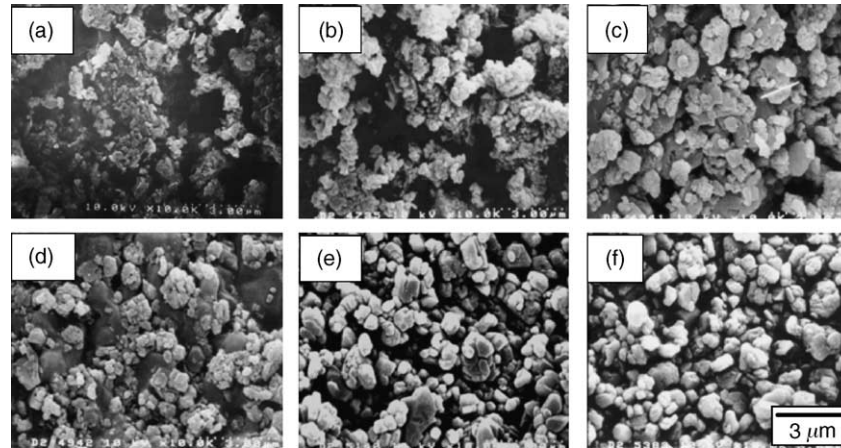
Fig. 10. Microstructure variations of α-LiAlO$_2$ mixture treated with molten carbonate at 650 °C: (a) initial, (b) 200, (c) 500, (d) 1000, (e) 2000 and (f) 3000 h.

by the phase transformation and solubility of LiAlO$_2$. Though LiAlO$_2$ is known to undergo an allotropic transformation in molten carbonate at around 650 °C [2,10], the phenomena has not been observed in the present study. This due to of the kinetics that are involved in the activation for the phase transformation. Terada et al. [1] have pointed out that Li$^+$ ions are dissolved from LiAlO$_2$, accordingly to the following reaction:

$$LiAlO_2 + O^{2-} \rightarrow Li^+ + AlO_3^{3-} \tag{1}$$
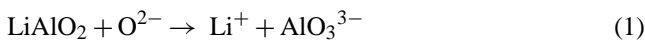
As can be seen in Figs. 1 and 2, LiNaCO$_3$ is precipitated out in the early stages of heat-treatment. It is also noteworthy that the elution of LiNaCO$_3$ does not occur in pure α-LiAlO$_2$
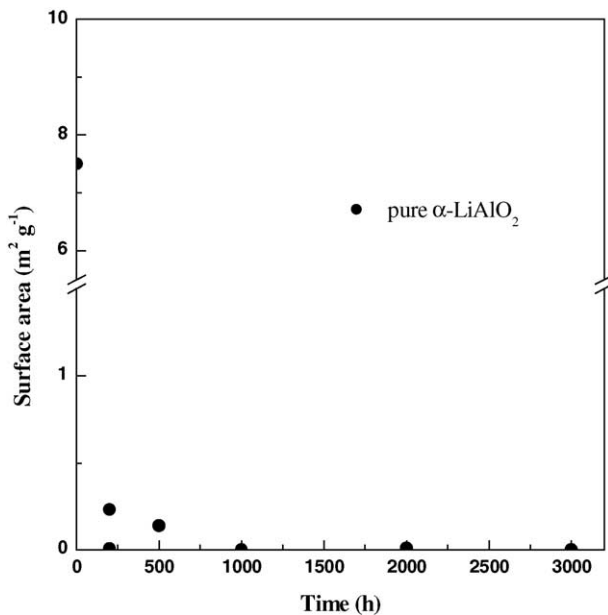

Fig. 11. Surface area variations of α-LiAlO$_2$ treated with molten carbonate at 650 °C as a function of treatment time.

(Fig. 4). Therefore, it is confirmed that LiNaCO$_3$ is synthesized by dissolved Li$^+$ ions from γ-LiAlO$_2$. The continuous dissolution of Li$^+$ ions from γ-LiAlO$_2$ is accelerated after 10 000 h, and it is reflected in the relative intensity ratio of α-LiAlO$_2$ over γ-LiALO$_2$ from an immersion test of an α-/γ-LiAlO$_2$ mixture (Fig. 3). By contrast, the elution rate of LiNaCO$_3$ from pure γ-LiAlO$_2$ (see Fig. 1) is maintained at an almost constant value. This can be explained by the nucleation and the growth of dissolved Li$^+$ ions from LiAlO$_2$. The dissolved Li$^+$ ions are thought to be used for both the elution of LiNaCO$_3$ and the nucleation and the growth of LiAlO$_2$. Terada et al. [2] reported that the dissolved Li$^+$ ions from γ-LiAlO$_2$, precipitate as α-LiAlO$_2$, which has a lower solubility. In the case of coexistence of γ-LiAlO$_2$ with α-LiAlO$_2$, the dissolved Li$^+$ ions from γ-LiAlO$_2$ can be easily deposited as α-LiAlO$_2$ via heterogeneous nucleation and growth. In this study, the dissolved Li$^+$ ions precipitate spontaneously as LiNaCO$_3$ and α-LiAlO$_2$. Therefore, as can be seen in Fig. 2, the intensity of LiNaCO$_3$ increases and the intensity of γ-LiAlO$_2$ decreases with heat-treatment time. For pure γ-LiAlO$_2$, however, the dissolved Li$^+$ ions can hardly be precipitated as α-LiAlO$_2$ in the absence of stable seed crystal (α-LiAlO$_2$). This is simply used for the construction of LiNaCO$_3$. Therefore, the concentration of Li$^+$ ions in the molten carbonate is so high that the dissolution of Li$^+$ ions from the LiAlO$_2$ is restricted by the saturation of equilibrium concentration.

It is also considered that the particle growth of LiAlO$_2$ is accelerated due to the dissolution and precipitation of lithium aluminate. Particles that have a large curvature or high solubility dissolve and precipitate as a stable form and have small surface area and low solubility are preferred. Therefore, as depicted in Figs. 7 and 8, the particle growth rate of an α-/γ-LiAlO$_2$ mixture is superior to that of pure γ-LiAlO$_2$, and the surface of the particles is smoothed out with continued heat-treatment time. The tendency of the surface area to decrease also indicates the rate of particle growth (Fig. 6). After

10 000 h, the particle growth of an α-/γ-LiAlO$_2$ mixture is faster by the accelerated dissolution and precipitation of Li$^+$ ions as a result of a solubility difference. Consequently, α-LiAlO$_2$ is considered to be stable in molten carbonate because the crystalline phase and the microstructure do not change during a 3 000 h immersion test. The reason why the surface area of α-LiAlO$_2$ decreases immediately after heat-treatment should be investigated.

5. Conclusions

The long-term stability of LiAlO$_2$ in molten carbonate at 650 °C in an air atmosphere has been examined for 18 000 h. From the early stages of heat-treatment, Li$^+$ ions are dissolved from γ-LiAlO$_2$, which has a high solubility in molten carbonate, and precipitated as LiNaCO$_3$ or α-LiAlO$_2$ which have low solubility. The particle growth of LiAlO$_2$ also originates through the dissolution and precipitation of lithium aluminate. Nevertheless, the particle size, the surface area and the crystalline phase of α-LiAlO$_2$ do not change during a 3000 h immersion test. These results show that α-LiAlO$_2$ has low solubility and is little decomposed in molten carbonate. It is therefore, an appropriate material for manufacturing MCFC matrices.

References

[1] S. Terada, I. Nagashima, K. Higaki, Y. Ito, J. Power Sources 75 (1998) 223–229.
[2] S. Terada, K. Higaki, I. Nagashima, Y. Ito, J. Power Sources 83 (1999) 227–230.
[3] J.Y. Cho, S.H. Hyun, J. Am. Ceram. Soc. 84 (5) (2001) 937–940.
[4] S.H. Hyun, S.C. Cho, J.Y. Cho, D.H. Ko, J. Mat. Sci. 36 (2001) 441–450.
[5] S.D. Kim, S.H. Hyun, T.H. Lim, S.A. Hong, J. Power Sources 137 (2004) 24–29.
[6] K. Takizawa, A. Hagiwara, J. Power Sources 109 (2002) 127–135.
[7] G.H. Fairchild, P.M. Brown, Proceedings of 1986 Fuel Cell Seminar, Tucson, AZ, 1986, pp. 239–243.
[8] R.A. Ribeiro, G.G. Silva, N.D.S. Mohallem, J. Phys. Chem. Solids 62 (2001) 857–864.
[9] V.S. Batra, S. Maudgal, S. Bali, P.K. Tewari, J. Power Sources 112 (2002) 322–325.
[10] K. Tanimoto, M. Yanagida, T. Kojima, Y. tamiya, H. Matsumoto, Y. Miyazaki, J. Power Sources 72 (1998) 77–82.